03

Hydrothermodynamics of water film, rivulets, and droplets on the surface of a streamlined body applying to the problem of icing

© A.V Kashevarov, A.L. Stasenko

Zhukovsky Central Aerohydrodynamic Institute,
Zhukovsky, Moscow oblast, Russia
e-mail: a.v.kash@yandex.ru

Received June 20, 2025
Revised September 2, 2025
Accepted October 14, 2025

The results of a physicomathematical and numerical analysis of the dynamics and heat transfer of liquid fragments entrained by an air flow along the surface of a solid are presented. The successive phenomena of film breakup into rivulets and of these rivulets into droplets are considered as a single process. An integral criterion, taking into account the total momentum of accelerating forces, is proposed to localize these breakups. The droplet freezing point is estimated based on the authors' previous work. The developed algorithm made it possible to predict the onset of icing on aircraft structural elements and the nature of the ice topography formed during flight conditions and ground experiments.

Keywords: Contact angle, surface tension, principle of minimum total energy, Young–Dupré, air-droplet flow, NACA0012 airfoil.

DOI: 10.61011/TP.2026.03.63154.155-25

Introduction

The motion of liquid films, rivulets, and droplets on the surface of a solid has long been investigated experimentally and theoretically in relation to various academic and applied problems. Reviews of studies focused on the problem of icing are indicative of a continuing interest in this phenomenon [1,2]. Specifically, the breakup of a film (formed, e.g., as a result of operation of an aircraft's thermal anti-icing system) flowing on the surface of a solid body alters significantly the growth rate and structure of ice forming downstream. In most studies, the dynamics of different fragments of liquid (films, rivulets, droplets) is considered separately or in pairs. In the present paper, we propose a physical and mathematical model that allows one to characterize the evolution of fragments of liquid of various sizes (from the breakup of a film to solidifying droplets) as a single process.

In general, the icing process is non-stationary and alters the shape of the object surface, which leads to a change in aerodynamic and thermal parameters on the surface. The stationary model proposed here provides an opportunity to calculate the flow of liquid along a surface and characterizes the probability of the onset of icing.

1. Analysis of the results preceding theoretical and experimental studies

The multidimensional space of flight parameter values (speed, cloud temperature, LWC (liquid water content, [g/m^3]), MVD (median volume diameter, [μm]) of droplets) has certain regions where ice is formed not in the vicinity of the leading edge of an airfoil, but as a result of slip and hardening of water fragments (film, rivulets, droplets) at hard-to-predict sites (runback ice), which makes it especially important to construct effective physical and mathematical models.

The corresponding numerical algorithms are often developed based on the principle of minimum total energy (MTE), which was originally proposed as a means of optimization of steam power plants [3].

Dimensionless parameter $X = b_r/b_f$, which is the ratio of transverse size $2b_r$ of the area wetted by a rivulet to width $2b_f$ of the film section that produced this rivulet, is introduced in MTE. The value of this ratio corresponding to the minimum of the sum of kinetic and potential energy is determined. The description of the latter can be traced back to the Young–Dupré equation for the surface energy density, which contains factor $(1 + \cos\theta)$, where θ is the wetting angle. Surface friction τ_a of gas flowing around the film and rivulet and tangential components of momentum of incident particles $\dot{m}_{\text{imp}}$, pressure gradient ∇p, and gravity force may be the active forces.

In the $\nabla p = 0$ case, the velocity profile in the film is linear (Taylor–Couette flow); in the contrary case, it is parabolic (Poiseuille flow). Pioneering MTE studies [3–5] were focused on film flow along a flat surface. Naturally, this approach, which was developed for a flat surface, is unsuitable for a profiled body on the spreading line of which τ_a and ∇p tend to zero.

The results of experimental studies of the flow around an airfoil (chord $L \approx 0.9$ m) were presented in [6]. Flow velocity $u_\infty \approx 90$ m/s, $T_\infty \approx -22\,^\circ$C, and MVD $= 20\,\mu$m. The thickness of a film was not measured; only the

coordinates of its decay line $s^*/L = 0.056$, $X \approx 0.4$ were recorded. The wetting angle was not specified.

A small-scale airfoil model ($L \approx 0.1$ m) was used in [7,8] to measure the thickness of a film at $u_\infty = 10-30$ m/s, $T_\infty = +20\,^\circ$C and image its breakup into rivulets, the number of which varied from one to ten within the specified limits of velocity variation. The s^*/L value remained within the range of $0.25-0.5$; the MVD of droplets was $10-50\,\mu$m.

The θ values were not specified in [6–8]. These experimental results were later subjected to theoretical analysis.

In [9], the data from [6] were processed under the assumption that $\theta = 68^\circ$ and the MVD of droplets is $20\,\mu$m. The film thickness was found to be $h_f \geq 5\,\mu$m. Despite the presence of a spreading line in experiments with an airfoil, the data from [7,8] were used in theoretical studies [10,11] that relied on the MTE principle. In addition, the influence of gradient ∇p was neglected. The first of these studies demonstrated the similarity of theoretical and experimental data at $\theta = 4^\circ$, while the second revealed an order-of-magnitude discrepancy in film thickness values (which is quite natural).

It follows from the analysis of these data that, compared to the values probed in experiments and the corresponding calculations, the MTE principle requires a significantly greater kinetic energy of translational motion of a film for it to break up.

The hydrodynamics of rivulets on an airfoil were examined in [12] within the ranges of $u_\infty = 10-30$ m/s, LWC $= 4.8-8.5$ g/m^3, $T_\infty = 22\,^\circ$C, and $\theta = (97 \pm 2)^\circ$. The relative width of rivulets was estimated at $X \approx 0.25-0.4$. The velocity profile in a film was assumed to be linear in mathematical modeling.

The surface density of the particle-film collision frequency in the above experiments may be estimated as

$$\dot{N} = \hat{\rho}_\infty \hat{u}_\infty / m_d = 10\,\mathrm{s}^{-1}\mathrm{m}^{-2}.$$

Naturally, the splashing of mass occurring when a supercooled droplet comes into contact with a thin „warm“ film and the propagation of disturbances potentially affecting the breakup of the film downstream constitute a complex three-dimensional non-stationary hydrodynamics problem. In power engineering, a similar problem for „warm“ droplets and films was discussed, e.g., in [13]. The problem of icing presents additional difficulties in description associated with crystallization and freezing of liquid fragments to the surface of a solid body. Experiments with airfoils with their chords differing by an order of magnitude indicate that the thicknesses of films produced by incident droplets and breaking up into rivulets are much smaller than those determined within MTE, which was developed for the case of a plate.

Thus, we failed to find a single published experimental study where the entire set of factors influencing the breakup of a film into rivulets (the angle of wetting of the body surface by water, variation of the velocity and thickness of the water film along the streamlined surface, the mass spectrum of incident droplets, the degree of turbulence of bearing air, and the surface microrelief) would be specified. Practical applications require a simple and convenient mathematical model adequate to the uncertainty of the physical scenario.

It bears reminding that the majority of theoretical and experimental studies are focused on film breakup into rivulets and the hydrodynamics of the latter on a vertical, horizontal, or inclined plane. Specifically, extensive experience accumulated in theoretical and experimental research into various icing regimes spurred the idea of using neural networks [14]. Papers [6–12] focused on the flow around straight airfoil models are directly related to aeronautics theory. However, the authors of these studies also did not consider the possibility of eventual formation of droplets from rivulets and their crystallization.

The interaction of a droplet with a solid substrate was examined at the molecular level in, e.g., [15].

2. Hydrothermodynamics of a film and rivulets

The proposed mathematical model characterizes the hydrothermodynamics of both the film and rivulets, which makes it a generalization of [16]. The following simplifying assumptions were made in its derivation:

— tangential stress τ_a for the film and rivulets is determined by calculations for a „dry“ airfoil;

— rivulets form and flow in those areas of the airfoil surface where the flux of incident droplets has already subsided (i.e, a new film does not form between the rivulets); and

— the influence of evaporation and the shear nature of liquid on the rate of its crystallization is neglected.

The diagram of flow of liquid fragments along the upper airfoil surface is shown in Fig. 1.

The hydrothermodynamics of the film (f) and the rivulet (r) are characterized by the following system of equations:

$$\rho_l \frac{d}{ds}\left(S_j^\perp \langle u_j \rangle\right) = \dot{m}_{\mathrm{imp}} 2b_j, \quad j \equiv f, r,$$

$$0 = -S_j^\perp \frac{dp}{ds} + \dot{m}_{\mathrm{imp}} \hat{v}_s 2b_j + \tau_a 2b_{aj} - \tau_w 2b_{wj}, \qquad (1)$$

$$\rho_l c_l \frac{d}{ds}\left(S_j^\perp \langle uT \rangle_j\right) = \dot{m}_{\mathrm{imp}}(c_l \hat{T} + \hat{V}^2/2)2b_f - q_a 2b_{aj} - q_w 2b_{wj}.$$

Here, $S_j^\perp = 2b_f h_f$ and $b_a = b_w = b_f$ for the film, while the rivulet has $\dot{m}_{\mathrm{imp}} = 0$, $S_r^\perp = R_r^2(\theta - \sin\theta\cos\theta)$, $b_{aj} = R_r\theta$, $b_{wj} = b_r = R_r \sin\theta$. Angular brackets $\langle\ \rangle$ denote averaging over the normal coordinate; $S_j^\perp$ is the cross section area; s is the longitudinal coordinate on the airfoil surface measured from the spreading line; $\dot{m}_{\mathrm{imp}}$ is the mass flux density of droplets that form the film; b_j is the half-width of the film region forming the rivulet or the line

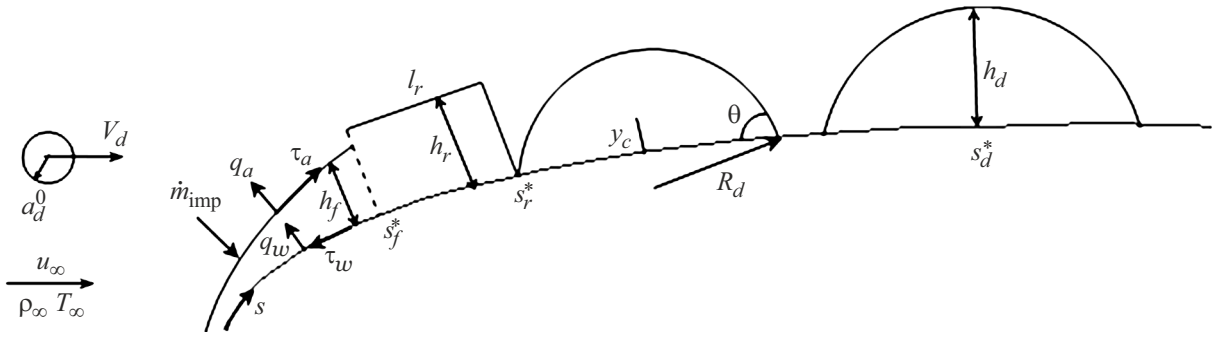

Figure 1. Geometry and hydrothermodynamics of a film (subscript f), a rivulet (r), and a droplet (d) on the surface of a streamlined body.

of contact between the rivulet and the surface; $\hat{V}$ and $\hat{v}_s$ are the velocity of a droplet and its longitudinal component at the point of impact; $\hat{T}$ is the droplet temperature; ρ_l, μ_l, and σ are the density, viscosity, and surface tension of water; and subscripts a, l, and f denote air, liquid, and film, respectively.

Icing starts when temperature T_j of the lower boundary of the film or rivulet reaches freezing temperature T_f. Icing rate $\partial h_i/\partial t$ may be determined from the heat balance condition: heat released during the phase transition must be transferred both into the film and into ice. Thus:

$$\frac{\partial h_i}{\partial t} = \begin{cases} 0, & T_l^- > T_f \\ (|q_l^+| + |q_l^-|)/\rho_i L_{ls} & T_l^- = T_f, \end{cases}$$

where q_l is the heat flux density from the lower boundary of the film into ice and L_i is the heat of the water–ice phase transition.

Icing rate $\frac{\partial h_i}{\partial t} = -\frac{\rho_l}{\rho_i}\frac{\partial h_l}{\partial t}$, h_l is included in the definition of $S_f^{\perp}$.

3. Estimation of the coordinates of film and rivulet breakup

A large number of studies focused on various types of film and rivulet instability and direct numerical calculation of the hydrodynamics of film breakup have already been published. In the present paper, we propose the W criterion: the ratio of the work of the sum of external factors (tangential surface tension and momentum of droplets penetrating into the film) to the total energy of surface tension:

$$b_f\left(\int_0^{s_f^*}\tau_\Sigma ds + \int_0^{s_{\text{imp}}}\dot{m}_{\text{imp}}\hat{v}_s ds\right) = (l_j\sigma + b_j\sigma_{ls})(1+\cos\theta)W$$

$$= b_r\int_{s_f^*}^{s_r^*}\tau_a ds,$$

$$\tau_\Sigma = \tau_a - h_f\nabla p. \qquad (2)$$

Here, $l_j \equiv b_f$ for the film; $l_j = R_r\theta$ for rivulets; s_f^* and s_r^* are the coordinates of film and rivulet breakup, respectively; and s_{imp} the limit coordinate of the airfoil region affected by incident droplets. A generalization of the Young–Dupré equation, which relates the parameters of three media, is adopted. The surface density of the energy of liquid–solid interaction is estimated as $\sigma_{ls} = 2\sqrt{\sigma\gamma_s}$, where $\gamma_s = 8.56\cdot 10^{-12}E_s$ [17] and E_s is the Young's modulus of the material of the streamlined solid body. It is clear that with absolute hydrophobicity ($\theta = \pi$), the film will break up (even if it starts to form) already in the vicinity of the spreading line on the airfoil.

The rivulet moves in the region of decreasing stress τ_a and increasing pressure gradient ∇p. The flow in it ceases as a result.

In the film/rivulet case under consideration, the critical W value may be determined by comparison with experimental data (e.g., [6,7]). Naturally, the active force is τ_Σ (2).

As was already noted, the kinetic energy of longitudinal motion of a thin film on the surface of a profiled airfoil in experiments [6–8] turns out to be an order of magnitude lower than that determined within the MTE, and the measured values of b_f^* and R_r are significantly greater than those predicted by these principles. This may be attributed, e.g., to disturbances introduced by uncontrolled turbulence of the external flow, bombardment by incident droplets, roughness of the surface of the streamlined body, etc. As a result, the forces entraining the film produce transverse instability of counter flows within the $-b_f^* < \Delta z < b_f^*$ region, which enter the rivulet. The width of the film section producing the rivulet may then be estimated from dimension considerations:

$$\frac{\rho_l}{\sigma}\left(\frac{\tau_a}{\mu_l}\right)^2 b_f^3 = (1+\cos\theta)c_f.$$

It follows from a comparison with experimental data [6,7] that the correction factor may be set equal to $c_f \approx 4\pi$. Since the film breakup occurs far from the flow stagnation line on the profile, the above Eqs. (1), (2) are supplemented by the following geometric relations [3–5].

The ratio of the width of the line of contact of the rivulet with the body surface to the width of the film producing

the rivulet is

$$X = \frac{\sin\theta}{\varphi(\theta)}\left[\frac{H^* g(\theta)}{2\theta/\sin\theta - \cos\theta}\right]^{2/3},$$

$$H^* = \frac{\rho_l}{\sigma}\left(\frac{\tau_\Sigma}{\mu_l}\right)^2 (b_f^*)^3 \sim 1 - \cos\theta, \qquad (3)$$

the radius of the cross section of the rivulet (circle segment) at the moment of formation is

$$R_r = b_f^*\left[\frac{\sin\theta}{\varphi(\theta)X}\right]^{1/2}, \qquad (4)$$

the width of the film section producing the rivulet is

$$2b_f = 2R_r \sin\theta/X,$$

and auxiliary functions are

$$g(\theta) = -\frac{1}{4}\cos^3\theta - \frac{13}{8}\cos\theta + \frac{15}{8}\frac{\theta}{\sin\theta} - \frac{3}{2}\theta\sin\theta,$$

$$\varphi(\theta) = \sin\theta - \frac{1}{3}\sin^3\theta - \theta\cos\theta.$$

4. Hydrodynamics of a droplet on the surface of a solid body

The hydrothermodynamics of droplets sliding along the surface of a plate were discussed in detail in [18,19]. The results reported there may be carried over to regions of a profiled airfoil with small curvature. We do not recapitulate here the formulations of physical and mathematical models presented in these studies and limit ourselves to numerical estimates.

A large number of papers focused on various types of rivulet instability on the surface of a solid in a gas flow have already been published [20,21]. The simplest solution was provided recently in [22]: it was demonstrated experimentally that the breakup of a rivulet on a substrate is governed (within the measurement error) by the classical Plateau–Rayleigh instability:

$$2\pi R_r/l_{rd} \approx 0.7,$$

where R_r is the radius of the cross section of the rivulet, which is assumed to be a segment of a circle, and l_{rd} is the wavelength of instability, which may be defined as the section of the rivulet that produces the initial droplet.

The latter is a three-dimensional object with a small area of contact with air and a small cross-sectional area. Neither surface friction nor drag force is sufficient to initiate its motion. Therefore, it remains stationary and continues to draw water from the rivulet until its size and the corresponding aerodynamic force become sufficient to overcome the force of interaction with the solid surface. The condition of equality of these forces yields an estimate of time τ_d of „filling“ of a droplet with water:

$$\tau_d = \frac{2}{3}\frac{a_d^3}{b_f h_f \langle u_f\rangle}. \qquad (5)$$

The radius of a sphere segment representing a sliding droplet equivalent in volume to a spherical droplet with radius a_d is

$$R_d = a_d\left[1 - (1+\cos\theta)^2(2-\cos\theta)/4\right]^{-1/3},$$

the cross-sectional area of a rivulet or droplet ($j \equiv r, d$) is

$$S_j^\perp = R_j^2(\theta - \sin\theta\cos\theta),$$

the height of a rivulet or droplet is

$$h_f = R_f(1 - \cos\theta),$$

the height of the center of the cross-sectional area of a droplet above the surface of a solid body is

$$y_c = \frac{R_d(\sin\theta - \theta\cos\theta - \sin^3\theta/3)}{\theta - \sin\theta\cos\theta},$$

and

$$b_j = R_j\sin\theta.$$

A droplet born at point s_r^* travels over a certain distance, and its base reaches freezing temperature T° at point s_d^*. The stopped droplet then goes through three stages: cooling of the entire mass to temperature T° within characteristic time τ_T, drawing the heat of phase transition L_{ls} off it at constant temperature $T_d = T^\circ$ within time τ_{ls}, and cooling of the formed ice particle within time τ_i. Since the ratio of the thermal conductivity coefficients of a solid, water, and air is written as $\lambda_w \gg \lambda_l \gg \lambda_a$, we obtain

$$\tau_T \sim a_d^3/(3R_d\chi_l). \qquad (6)$$

Next,

$$\tau_{ls} \sim \frac{L_{ls}}{c_l(T^\circ - T_a)}\frac{a_d^3}{3R_d\chi_{ls}},\ \ \tau_i \sim \tau_T\chi_l/\chi_i, \qquad (7)$$

where $\chi_j = \lambda_j/(\rho_j c_j)$ is the thermal diffusivity of the material ($j \equiv l, i$).

Since the mass of crystallizing water varies with time, χ_{ls} may be taken as the average between χ_l and χ_i. Numerical estimates of these times are given below.

In real practice, both the oncoming flow and the boundary layer are characterized by a certain degree of turbulence. This should lead to dispersal of both the rivulets emerging at the end and the droplets that solidify and freeze to the surface.

Following [23,24], we assume that the droplet slides along the surface without rotating within the examined range of θ values.

Thus, the proposed model allows one to predict the sites of runback ice formation on the surface of the airfoil.

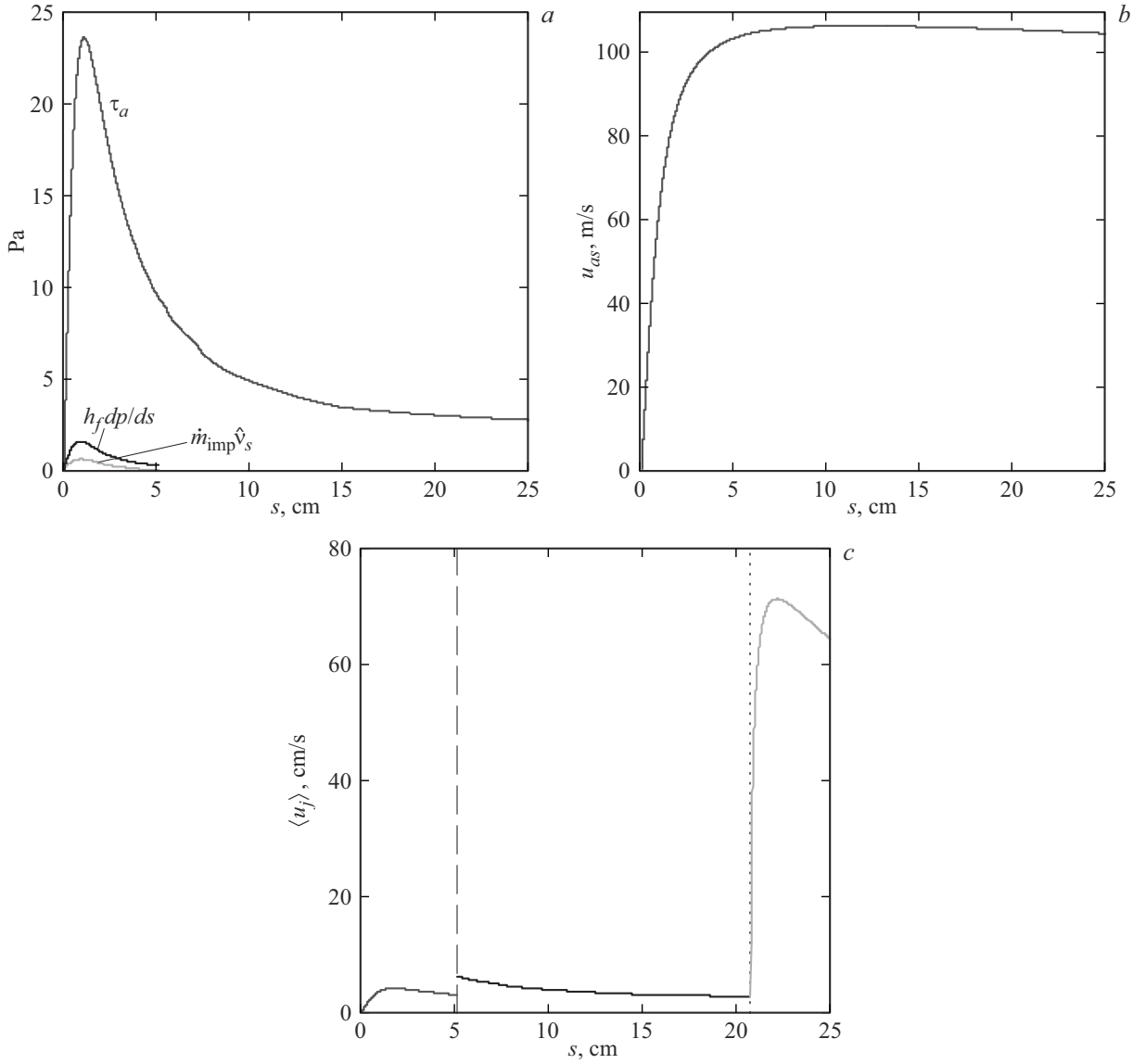

Figure 2. Longitudinal distributions: *a* — friction stress on the outer surface of the film and flux densities of the pressure pulse and incident droplets; *b* — air velocity at the outer edge of the boundary layer; *c* — water fragment velocity.

5. Example of a numerical study

Numerical studies were performed for the NACA0012 airfoil with defining parameters [6] and chord $L = 0.9$ m; $u_\infty = 90$ m/s, $T_\infty = -22\,^\circ$C, LWC $= 0.55$ g/m^3, and MVD $= 20\,\mu$m. Tabular data on the physical and mechanical characteristics of water, ice, and steel, which covered the nose of the profile, were used to obtain numerical estimates. Contact angle θ was taken equal to 90°, and $L_{ls} = 3.5 \cdot 10^5$ J/kg.

Local density of incident particles $\hat{\rho}$ and normal $\hat{v}_n$ and tangential $\hat{v}_\tau$ components of their velocity at the point of impact are determined by known algorithms [25]. The temperature of incident particles may be considered equal, within a small percentage, to the flow temperature, $\hat{T} \approx T_\infty$. The air flow is considered to be laminar.

The goal of modeling is to characterize icing of a streamlined surface. There are several obvious scenarios here; for example, if the film has enough time to solidify before breakup into rivulets, there is no need to examine the history of rivulets and droplets. This precedence has an undoubted influence on further development of the ice relief. Film solidification was discussed in [16].

The solidification of a rivulet on an inclined plane has been studied experimentally and theoretically for at least one and a half centuries. One relatively recent example is study [26].

In the present calculations, we consider flow conditions under which neither the film nor the rivulets start to solidify. In this case, the examination of their dynamics and heat exchange serves only to determine the initial conditions for the droplets forming during the breakup of rivulets.

The dependences of τ_a and ∇p (Fig. 2, *a*) on tangential coordinate are calculated for the case of a „dry“ profile, since the gas velocity is much greater than the velocity

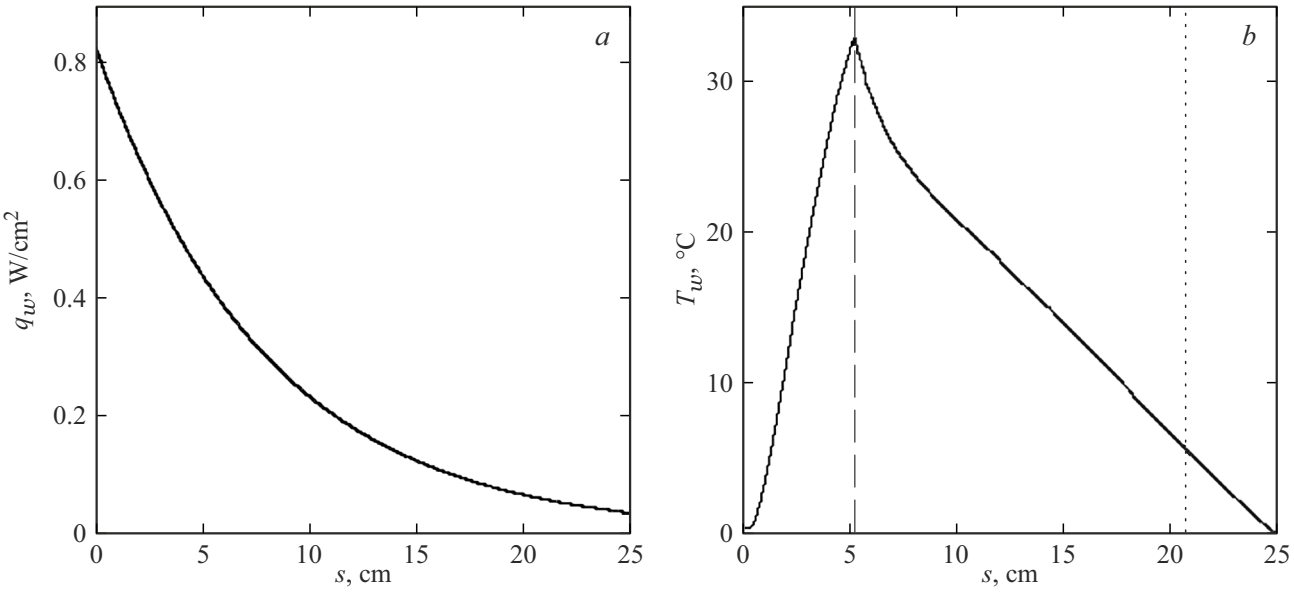

Figure 3. Longitudinal distributions: a — density of the heat flux into the film; b — surface temperature of the streamlined body.

of the film, liquid, and droplets, which allows them to be considered stationary, and their small thickness alters the profile shape only slightly. It is clear that the main force entraining the film is air friction τ_a. Thus, the velocity profile in the film may be considered linear.

Figure 2, b shows the air velocity above the boundary layer surface on the airfoil.

Dashed and dotted lines in Fig. 2, c indicate coordinates s_f^*, s_r^* of film breakup into rivulets and rivulet breakup into droplets, which were obtained according to (2) under the assumption that $W = 0.6$. In this case, the value of s_f^* is almost the same as the result of processing the experimental data from [6] in [9] (Table 2).

The distribution of heat flux $q_w(s)$ (Fig. 3, a) associated with the operation of the heater was set along the profile contour, and the surface temperature (Fig. 3, b) was determined by solving the corresponding systems of equations. It can be seen from Fig. 3, b that the produced rivulet cools down rapidly after the breakup of the film. Following the rivulet breakup, the surface temperature is extrapolated to the freezing temperature.

Figure 4 presents the distributions of film thickness and maximum rivulet and droplet height along the profile contour. The circle denotes the maximum droplet height at the very moment of breakup of the rivulet (when the droplet cannot yet start to move under the influence of aerodynamic forces). The droplet starts to move when its height reaches a value on the order of $100\,\mu$m.

The dashed line is the half-width of the film section that produces the rivulet. With the adopted value of $\theta = 90°$, we have (4) $R_r = h_r > b_f$; thus, the droplets produced by neighboring rivulets could merge even before freezing. Presumably, this is prevented in practice by the non-simultaneity of separation of droplets from rivulets and the turbulence of air flow that entrains the rivulets and droplets.

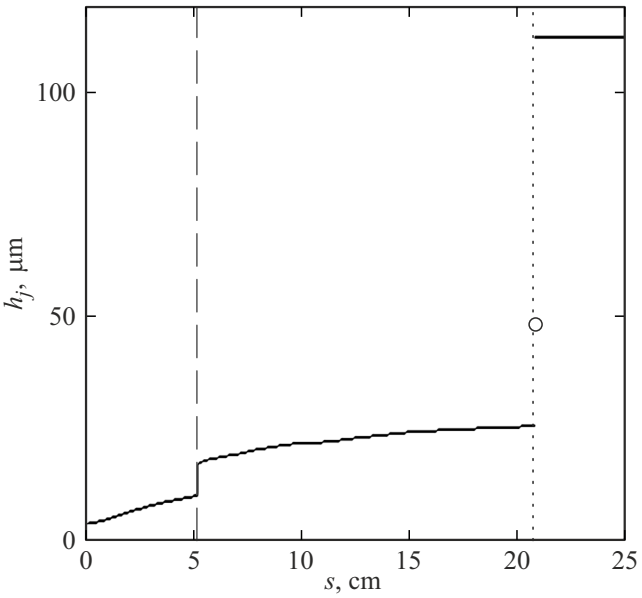

Figure 4. Longitudinal distributions of water film thickness, rivulet height, and droplet height ($j \equiv f$, r, d, respectively).

Thus, determined were the critical points of film and rivulet breakup and droplet freezing; ratio (3) of the width of the rivulet and the section of the film that produced it $X = 0.5$; radius $a_d = 90\,\mu$m of the volume-equivalent droplet; and period of droplet detachment from the rivulet $\tau_d \sim 0.1$ s (5).

Estimates of the characteristic scales yield droplet cooling time (6) $\tau_T \sim 6$ ms; the droplet crystallization and solidification (7) times are $\tau_{ls} \sim 100$ ms and $\tau_I \sim 10$ ms.

Even the classical experiments discussed in [27] make it clear that the degree of longitudinal velocity pulsations may reach $\sim 10\,\%$, while transverse pulsations are two times

less intense. The advances in turbulent boundary layer theory have already been incorporated into standard codes used in icing studies. Thus, the localization of a frozen droplet is actually not strictly determined: instabilities of rivulets [20] may already lead to scattering of detached droplets, and turbulence of the carrier flow may induce their two-dimensional random walk. This is the subject of a separate study.

Conclusion

An algorithm for approximate characterization of the process of film breakup up to the point of solidification of droplets formed from rivulets on the surface of a solid in a supercooled air flow was presented. The proposed approach circumvents the complications inherent in the commonly used principle of minimum total energy, which is inapplicable in the vicinity of the spreading line on an airfoil or the stagnation point on a blunt body. Despite the heuristic nature of certain assumptions, the numerical results obtained for a flow around a straight airfoil were proven reliable by comparing them with data from published theoretical and experimental studies. Specifically, It was demonstrated that the surface roughness induced by solidified droplets under typical flow conditions in terrestrial experiments may reach a height on the order of tenths of a millimeter, exerting a significant influence on the regime of flow around the airfoil.

This approach may be used in non-stationary icing models that take variations of the surface shape during ice growth into account. In addition, it provides an opportunity to develop a flight algorithm for estimating the power of preemptive heating of the leading airfoil edge (using the data on cloud parameters along the flight path; see, e.g., [28]) for prevention of the formation of runback ice.

Conflict of interest

The authors declare that they have no conflict of interest.

References

[1] M. Yamazaki, A. Jemcov, H. Sakaue. J. Airspace, **8** (7), 188 (2021). DOI: 10.3390/aerospace8070188
[2] J. Mora, P. García, F. Carreño, M. González, M. Gutiérrez, L. Montes, V.R. Gavira, C. López-Santos, A. Vicente, P. Rivero, R. Rodríguez, S. Larumbe, C. Acosta, P. Ibáñez-Ibáñez, A. Corozzi, M. Raimondo, R. Kozera, B. Przybyszewski, A.R. González-Elipe, A. Borrás, F. Redondo, A. Agüero. Surf. Coatings Technol., **465**, 2023129585 (2023). DOI: 10.1016/j.surfcoat.2023.129585
[3] J. Mikielewiecz, J.R. Moszynski. Intern. J. Heat Mass Transfer, **19** (7), 771 (1976). DOI: 10.1016/0017-9310(76)90130-7
[4] T. Hobler. Chemia Stosowana B, **2**, 145 (1964).
[5] S.G. Bankoff. Intern. J. Heat Mass Transfer, **14** (12), 2143 (1971). DOI: 10.1016/0017-9310(71)90034-2
[6] K.M. Al-Khalil, C. Horvath, D.R. Miller, W. Wright. NASA TM 2001–210907 (2001). DOI: 10.2514/6.1997-51
[7] K. Zhang, B. Johnson, A.P. Rothmayer, H. Hu. AIAA, 2014–0741 (2014). DOI: 10.2514/6.2014-0741
[8] K. Zhang, T. Wei, H. Hu. Exp. Fluids, **56** (9), 173 (2015). DOI: 10.1007/s00348-015-2046-z
[9] G.A.L. Silva, O.M. Silvares, E.J.G.J. Zerbini. AIAA, 2006–3785 (2006). DOI: 10.2514/6.2006-3785
[10] W. Dong, M. Zheng, J. Zhu, G. Lei. J. Aircraft, **53** (6), 1597 (2006). DOI: 10.2514/1.C033637
[11] A. Gosset. EUCASS 2017–482 (2017). DOI: 10.13009/EUCASS2017-482
[12] Y. Lou, X. Bu, X. Shen, G. Lin, R. Zhang, F. Zeng, H. Jin, K. Ma, D. Wen. Aerospace, **9** (10), 570 (2022). DOI: 10.3390/aerospace9100570
[13] M.E. Deich, G.A. Filippov. *Gazodinamika dvukhfaznykh sred* (Energoizdat, M., 1981) (in Russian)
[14] E. Ogretim, W. Huebsch, A.F. Shinn. J. Aircraft, **43** (1), 233 (2006). DOI: 10.2514/1.16241
[15] S.Sh. Rekhviashvili, A.A. Sokurov. Tech. Phys., **69** (4), 522 (2024). DOI: 10.61011/JTF.2024.04.57525.267-23
[16] A.V. Kashevarov, A.L.Stasenko. Thermophys. Areromechan., **26** (2), 223 (2019). DOI: 10.1134/S0869864319020069
[17] J.J. Gilman. J. Appl. Phys., **31** (12), 2208 (1960). DOI: 10.1063/1.1735524
[18] E.S. Grinats, A.B. Miller, A.L. Stasenko, V.A. Zhbanov, A.V. Kashevarov, Y.F. Potapov. High Temp., **57** (2), 222 (2019). DOI: 10.1134/S0018151X19020056
[19] V.A. Zhbanov, A.L Stasenko, O.D. Tokarev. High Temp., **60** (6), 791 (2022). DOI: 10.1134/s0018151x22060086
[20] G.W. Young, S.H. Davis. J. Fluid Mech., **176**, 1 (1987). DOI: 10.1017/S0022112087000557
[21] A. Daerr, J. Eggers, L. Limat, N. Valade. Phys. Rev. Lett., **106** (18), 184501 (2011). DOI: 10.1103/PhysRevLett.106.184501
[22] M. Hartmann, M. Fricke, L. Weimar, D. Gründing, T. Marié, D. Bothe, S. Hardt. Intern. J. Multiphase Flow, **140**, 103582 (2021). DOI: 10.1016/j.ijmultiphaseflow.2021.103582
[23] J. Xie, J. Xu, W. Shang, K. Zhang. Intern. J. Heat Mass Transfer, **122**, 45 (2018). DOI: 10.1016/j.ijheatmasstransfer.2018.01.098
[24] M. Backholm, D. Molpeceres, M. Vuckovac, H. Nurmi, M.J. Hokkanen, V. Jokinen, R.H. Ras. Commun. Mater., **1** (1), 64 (2020). DOI: 10.1038/s43246-020-00065-3
[25] A.Y. Varaksin. High Temp., 56 (2), 275 (2018). DOI: 10.1134/S0018151X18020220
[26] A. Huerre, A. Monier, T. Séon, C. Josserand. J. Fluid Mech., **914**, A32 (2021). DOI: 10.1017/jfm.2021.41
[27] H. Schlichting. *Grenzschicht-Theorie* (Verlag G. Braun, Karlsruhe, 1964)
[28] L. West, G. Gimmestad, R. Herkert, W. Smith, S. Kireev, T. Daniels, L. Cornman, B. Sharman, A. Weekley, G. Perram, K. Gross, G. Smith, W. Feltz, J. Taylor, E. Olson. AIAA, 2009–3635 (2009). DOI: 10.2514/6.2009-3635

Translated by D.Safin